RSC Mechanochemistry

ROYAL SOCIETY OF CHEMISTRY

PAPER

View Article Online
View Journal

Cite this: DOI: 10.1039/d6mr00040a

Mechanistic insights into mechanochemical oxidation of 1,1-disubstituted alkenes mediated by polymer-derived mechanoradicals

Akira Kodaka,[a] Takumi Yamamoto,[a] Hajime Sugita,[a] Akira Takahashi [a] and Hideyuki Otsuka *[ab]

Polymer-derived mechanoradicals generated under solid-state conditions offer a unique platform for driving chemical transformations that are difficult to achieve in solution. Here, we report a mechanoradical-mediated oxidation of 1,1-disubstituted alkenes using a polymer as the radical source and molecular oxygen as the oxidant. Ball milling of polystyrene (PS) in the presence of diarylethene (DAE) derivatives under air resulted in backbone cleavage of PS in addition to oxidative cleavage of the alkene moiety to afford the corresponding diaryl ketone (DAK) derivatives. Electron paramagnetic resonance (EPR) spectroscopy revealed the formation of oxygen-centered radical species, suggesting a reaction pathway involving the addition of mechanoradicals derived from PS to DAE, followed by reaction with molecular oxygen. The experiments using poly(methyl methacrylate) (PMMA) instead of PS gave similar results, indicating that the oxidative cleavage proceeds irrespective of the polymer species. Gel permeation chromatography with a UV detector further supported the addition of PMMA-derived mechanoradicals to DAE derivatives. Substituent effect studies showed that DAK formation occurs for DAE derivatives with both electron-donating and electron-withdrawing substituents, whereas oxirane derivatives (DAO) were observed only for derivatives with electron-withdrawing groups, reflecting substituent-dependent stability of DAO. These findings establish polymer-derived mechanoradicals as effective initiators for alkene oxidation in the solid state and demonstrate the potential of mechanochemistry as a powerful platform for elucidating radical oxidation mechanisms under solvent-free conditions.

Received 31st March 2026
Accepted 22nd May 2026

DOI: 10.1039/d6mr00040a

rsc.li/RSCMechanochem

Introduction

Oxidative cleavage reactions are one of the fundamental reactions in organic chemistry, in which carbon–carbon double bonds (C=C) are cleaved by oxidation to generate carbonyl compounds, such as ketones and aldehydes. These reactions are widely employed in organic synthesis and play a central role in total synthesis and pharmaceutical synthesis.[1–5] Traditionally, oxidative cleavage reactions have relied on the use of strong oxidants, including ozone,[6] potassium permanganate,[7] and ruthenium-based oxidants,[8,9] many of which suffer from drawbacks related to safety, toxicity, and environmental impact.[10–13] Consequently, the development of more environmentally benign oxidative methods has attracted increasing attention, and the use of molecular oxygen (O_2) as an oxidant has emerged as an appealing alternative.

In recent years, oxidative cleavage of alkenes using molecular oxygen has been achieved through radical-mediated catalytic processes.[14–27] Representative radical sources include *N*-hydroxyphthalimide (NHPI),[14–16] 2,2,6,6-tetramethylpiperidin-1-oxyl (TEMPO),[17] thiols or disulfides,[18–20] and 2,2′-azobisisobutyronitrile (AIBN).[21–23] However, reports on the formation of synthetically important products such as epoxides remain limited,[16,22,23] and the underlying reaction mechanisms are not yet fully understood.

Along with the development of polymer mechanochemistry, studies exploiting so-called mechanoradicals, radical species generated by homolytic scission of polymer backbones under mechanical stimuli, for polymer modification and the detection of chain scission events have been actively pursued.[28,29] To date, mechanoradicals have been utilized for self-strengthening gels,[30–32] the introduction of fluorescence properties,[33–35] and the elucidation of fracture mechanisms in polymeric materials.[36–39] In contrast, despite their unique reactivity, the application of polymer-derived mechanoradicals to the transformation of low-molecular-weight compounds remains largely unexplored, with only a single example reported to date,[40] to the best of our knowledge.

[a]*Department of Chemical Science and Engineering, Institute of Science Tokyo, 2-12-1 Ookayama, Meguro-ku, Tokyo 152-8550, Japan. E-mail: otsuka@mac.titech.ac.jp*
[b]*Research Center for Autonomous Systems Materialogy (ASMat), Institute of Integrated Research, Institute of Science Tokyo, 4259 Nagatsuta-cho, Midori-ku, Yokohama, Kanagawa 226-8501, Japan*

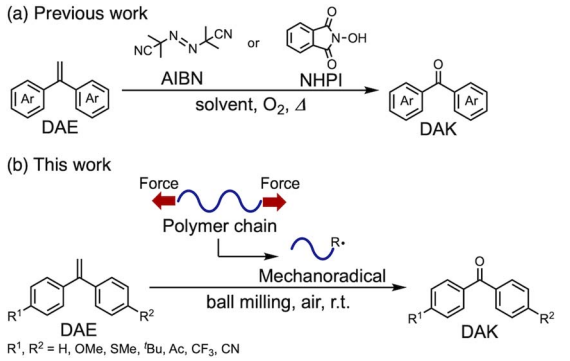

Scheme 1 (a) Conventional solution-phase oxidative cleavage of 1,1-disubstituted alkenes using molecular oxidants. (b) Polymer-derived mechanoradical-mediated oxidative cleavage of DAE derivatives under solvent-free solid-state conditions (this work).

A defining feature of mechanochemical reactions is that they proceed in the solid state. In the absence of solvent, reactive species and catalysts are free from solvation and diffusion effects that are characteristic of solution-phase reactions. Such reaction environments can stabilize reactive intermediates or transition states that are otherwise difficult to observe in solution, thereby providing a powerful platform for gaining mechanistic insight.[41–43] Moreover, solid-state reactions minimize solvent usage, simplify reaction systems, and often exhibit favourable energy efficiency compared with photochemical or thermal reactions.[43–45] From this perspective, polymer-derived mechanoradicals offer a promising and environmentally benign approach for exploring new reaction systems.

In this study, we aimed to expand the scope of transformations of low-molecular-weight compounds driven by mechanoradicals generated under solid-state conditions. As a model system, we focused on 1,1-diarylethene (DAE) derivatives, a representative class of 1,1-disubstituted alkenes, and investigated their mechanochemical oxidative cleavage using polymer chains as a radical source and atmospheric oxygen as the oxidant (Scheme 1). The radical intermediates generated during the solid-state reactions were characterised by electron paramagnetic resonance (EPR) spectroscopy, while the structural evolution of the closed-shell intermediates and products was analysed by nuclear magnetic resonance (NMR) spectroscopy and gel permeation chromatography (GPC). Through this approach, we elucidated the reaction mechanism of radical-mediated oxidative cleavage of 1,1-disubstituted alkenes within solid polymer matrices and demonstrated the potential of mechanochemical reactions as a versatile platform for mechanistic analysis.

Results and discussion

To investigate whether oxidative cleavage reactions can be induced by mechanoradicals generated upon polymer chain scission, a mixture of 1,1-bis(4-methoxyphenyl)ethene (**DAE-OMe/OMe**) and polystyrene (PS) was subjected to ball milling. ^{1}H NMR analysis of the milled sample revealed the emergence of new signals that were not attributable to either **DAE-OMe/OMe** or

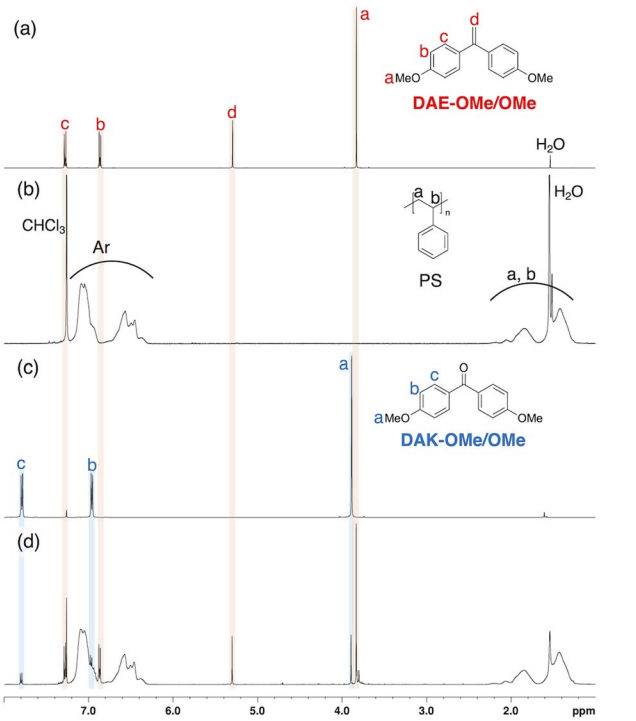

Fig. 1 ^{1}H NMR spectra of (a) **DAE-OMe/OMe**, (b) PS, (c) **DAK-OMe/OMe** and (d) a ground mixture of **DAE-OMe/OMe** and PS ($CDCl_3$, 500 MHz).

PS (Fig. 1). These signals were consistent with those of the corresponding diaryl ketone (DAK) derivative (**DAK-OMe/OMe**), the oxidative cleavage product of **DAE-OMe/OMe**, indicating that oxidative cleavage had occurred under the milling conditions. Notably, the isolated yield of **DAK-OMe/OMe** (29%) was in good agreement with the conversion of **DAE-OMe/OMe** calculated from the ^{1}H NMR spectrum of the milled mixture (32%), suggesting that the oxidative cleavage reaction proceeded with high selectivity under the applied reaction conditions.

GPC analysis before and after ball milling showed a significant decrease in the number-average molecular weight (M_n) of PS, confirming that polymer chain scission was induced by mechanical grinding, thereby generating mechanoradicals (Fig. 2).

To determine whether the formation of **DAK-OMe/OMe** originated from the polymer-derived mechanoradicals, a control experiment was conducted in which **DAE-OMe/OMe** was ball-milled in the absence of PS. As a result, only the signals of **DAE-OMe/OMe** were observed in the ^{1}H NMR spectrum (Fig. S61), indicating that no reaction occurred. These results demonstrate that a polymer-derived radical source is essential for the mechanochemical oxidative cleavage of DAE.

To further examine the involvement of radical species in the oxidative cleavage process, EPR measurements were performed before and after ball milling of a mixture of **DAE-OMe/OMe** and PS. As a control experiment, EPR spectra of PS alone were also recorded before and after milling. No EPR signals were detected for PS alone, whereas a distinct radical signal was observed only when **DAE-OMe/OMe** was present during ball milling (Fig. 3).

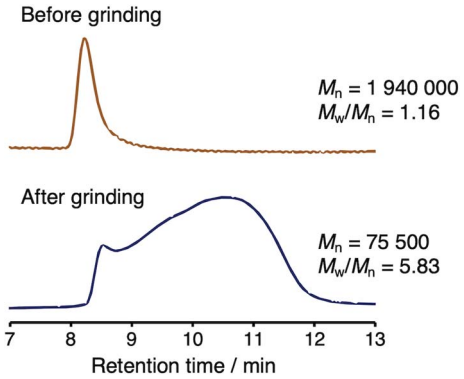

Fig. 2 GPC profiles of a mixture of PS and **DAE-OMe/OMe** before and after grinding (THF, RI).

The calculated g value of 2.0042 is characteristic of oxygen-centred radicals, consistent with the formation of relatively stable oxygen-centred radical species.

To evaluate the influence of reaction parameters on the mechanochemical oxidation reaction, the effects of ball-milling time, PS molecular weight, DAE loading, and the presence of molecular oxygen were examined under otherwise comparable conditions (Table 1). First, the dependence of the reaction on ball-milling time was investigated. When the milling time was shortened from 60 min to 30, 15, and 10 min, the ^{1}H NMR yields of the DAK product decreased to 14%, 9.9%, and 6.5%, respectively (entries 1–4). GPC analysis of the milled PS samples further showed that the molecular weight of PS decreased progressively with increasing milling time, indicating that polymer chain scission becomes more extensive during prolonged milling (Fig. S63). These results are consistent with the idea that longer milling times promote additional chain scission and thereby increase the number of polymer-derived radicals available for productive reaction with the DAE substrate.

Next, the effect of PS molecular weight was examined. When PS samples with different molecular weights were employed, the ^{1}H NMR yield of the DAK product increased with increasing polymer molecular weight. Specifically, PS with M_n = 792, 320, 38, and 6 kDa gave DAK yields of 17%, 13%, 6.9%, and 1.0%, respectively (entries 5–8). GPC analyses before and after ball milling showed that the extent of molecular-weight reduction became more pronounced as the initial molecular weight of PS increased, whereas PS with M_n = 6 kDa exhibited little change in its GPC trace after milling (Fig. S64–S67). These results

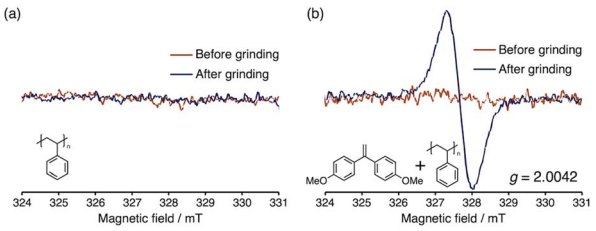

Fig. 3 EPR spectra of (a) PS alone before and after grinding and (b) a mixture of PS and **DAE-OMe/OMe** before and after grinding.

Table 1 Effect of reaction parameters on the mechanochemical oxidation reaction

Entry	PS M_n (kDa)	**DAE-OMe/OMe** (μmol)	Ball-milling time (min)	^{1}H NMR yield (%)
1	1940	50	60	29[a]
2	1940	50	30	14
3	1940	50	15	9.9
4	1940	50	10	6.5
5	792	50	60	17
6	320	50	60	14
7	38	50	60	6.9
8	6.0	50	60	1.0
9	1940	10	60	7.3
10	1940	25	60	7.6
11	1940	100	60	11
12	1940	500	60	1.1
13[b]	1940	50	60	3.5

[a] Isolation yield. [b] Under N_2-like conditions.

suggest that higher-molecular-weight PS undergoes more extensive chain scission under the present milling conditions, thereby generating a larger number of mechanoradicals and promoting more efficient reaction with the DAE substrate. The effect of substrate loading was also examined by varying the amount of **DAE-OMe/OMe** relative to PS (entries 9–12). Using 10, 25, 100, and 500 μmol of **DAE-OMe/OMe** gave ^{1}H NMR yields of 7.3%, 7.6%, 11%, and 1.1%, respectively, indicating that an intermediate substrate loading is optimal under the present conditions. At lower DAE loadings, productive trapping of polymer-derived radicals by the alkene substrate is likely less efficient, allowing competing pathways to become more significant. In contrast, at higher DAE loadings, the composition of the milling mixture may become less favorable for efficient polymer chain scission and productive radical generation.

Finally, the role of molecular oxygen was examined by carrying out the reaction under conditions designed to minimize exposure to O_2 (entry 13). Under these conditions, the ^{1}H NMR yield of the DAK product decreased markedly to 3.5%, indicating that molecular oxygen plays an essential role in the present transformation. This result supports the view that O_2 is involved not only as the terminal oxidant but also in key radical processes leading to product formation.

To further investigate the addition reaction of polymer-derived mechanoradicals to DAE derivatives, poly(methyl methacrylate) (PMMA) was employed in place of PS. Because PMMA does not absorb at 254 nm, it enables monitoring of the addition process by GPC with UV detection (λ = 254 nm). A mixture of PMMA and **DAE-OMe/OMe** was subjected to ball milling. ^{1}H NMR analysis of the reaction mixture revealed the formation of **DAK-OMe/OMe** as the major product, similar to the results obtained using PS (Fig. 4). These results indicate that mechanoradical-mediated oxidative cleavage proceeds regardless of the type of polymer. However, the ^{1}H NMR spectrum of the milled mixture showed that both the conversion of the DAE derivative (12%) and the NMR yield of the DAK derivative (8%) were lower than those observed with PS. This difference is attributed, at least in part, to the lower molecular weight of

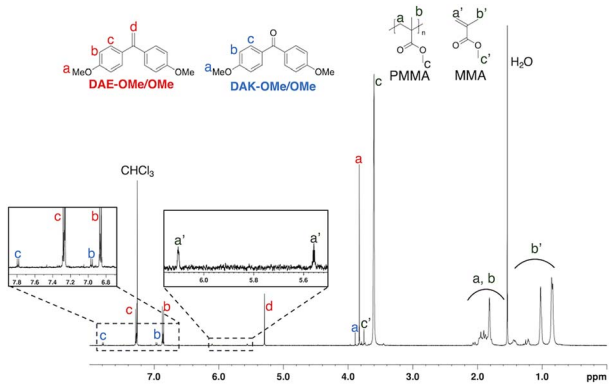

Fig. 4 ^{1}H NMR spectrum of a mixture of **DAE-OMe/OMe** and PMMA after grinding ($CDCl_3$, 500 MHz).

PMMA ($M_n = 1.4 \times 10^5$) compared to PS ($M_n = 1.9 \times 10^6$), which likely results in a reduced amount of mechanoradicals generated upon mechanical scission. In addition, signals attributable to methyl methacrylate (MMA) were observed in the ^{1}H NMR spectrum of the reaction mixture, suggesting that depolymerization of PMMA occurs under the milling conditions.[46] Accordingly, depolymerization processes mediated by polymer-derived mechanoradicals are likely to compete with the addition of mechanoradicals to DAE derivatives, thereby contributing to the reduced efficiency of the oxidative cleavage reaction.

GPC analysis before and after ball milling of PMMA with **DAE-OMe/OMe** using a refractive index (RI) detector showed that the M_n of PMMA decreased from 138 000 to 24 000, confirming mechanically induced cleavage of the PMMA chain (Fig. 5). Notably, GPC analysis using a UV detector ($\lambda = 254$ nm) revealed the emergence of polymer peaks ($M_n = 7900$) after ball milling of PMMA in the presence of **DAE-OMe/OMe**, whereas no such peaks were observed after ball milling of PMMA alone. Since PMMA itself does not absorb at 254 nm, these results indicate that mechanoradicals generated from PMMA added to **DAE-OMe/OMe**, resulting in the formation of polymer chains bearing DAE-derived structures at the chain ends.

On the basis of these results, a plausible mechanism for the mechanoradical-mediated oxidative cleavage of DAE derivatives is proposed as follows (Scheme 2). Under the present aerobic

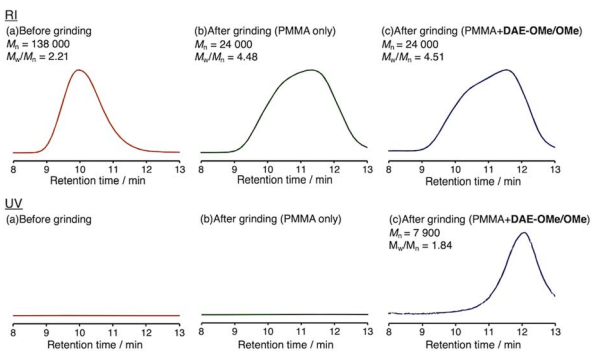

Fig. 5 GPC profiles of (a) PMMA before grinding, (b) PMMA after grinding and (c) a mixture of PMMA and **DAE-OMe/OMe** after grinding (THF).

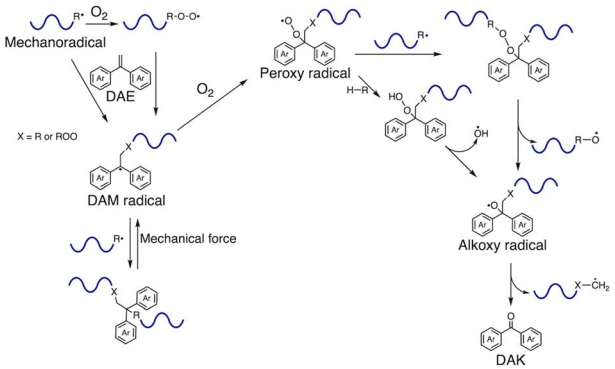

Scheme 2 Plausible mechanism for the reaction of DAE derivatives with mechanoradicals.

milling conditions, polymer-derived mechanoradicals and/or oxygen-trapped radical species may react with DAE derivatives to generate oxygenated radical intermediates. Subsequent radical processes, including oxygen addition, hydrogen abstraction, and fragmentation of alkoxy-type intermediates, are proposed to lead to the formation of the corresponding DAK derivatives. In this fragmentation step, release of the DAK product would concomitantly generate a polymer-end carbon-centered radical, which is considered to be chemically analogous to the initially formed mechanoradical and may therefore participate in subsequent radical processes under the milling conditions. A related fragmentation pathway, in which an alkoxy-type intermediate gives a carbonyl product together with a carbon-centered radical that undergoes further O_2 trapping and radical transformations, has also been proposed in the literature.[16] At present, however, the experimental data do not allow us to unambiguously identify the rate-determining step of the overall mechanism.

Although mechanochemical reactions under solvent-free conditions differ fundamentally from solution-phase reactions, substituent effects analogous to those observed in solution are sometimes observed.[47–49] To evaluate the substrate scope of the mechanoradical-mediated oxidative cleavage and to obtain further mechanistic insights, the effect of aromatic substituents on the reaction was investigated. A series of nine DAE derivatives bearing electron-donating or electron-withdrawing substituents at the para positions were

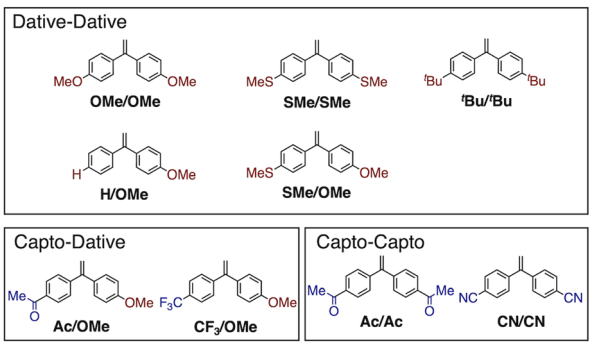

Fig. 6 Chemical structures of the investigated DAE derivatives.

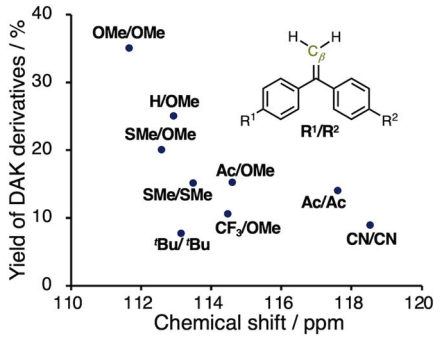

Fig. 7 Yield of DAK derivatives calculated from ^{1}H NMR spectra as a function of the chemical shift of β carbon of DAE derivatives in ^{13}C NMR spectra.

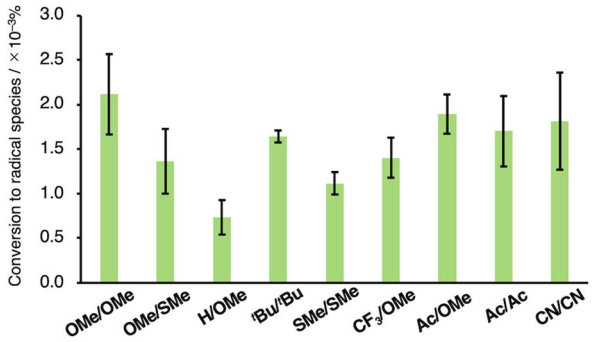

Fig. 9 Conversion ratio of DAE derivatives to radical species calculated based on EPR measurements.

synthesized, and their mechanochemical oxidative cleavage reactions were examined (Fig. 6). To enable a clear discussion of electronic effects, meta-substituted derivatives, for which the electronic influence is diminished, as well as ortho-substituted derivatives, which may introduce kinetic effects, were not investigated in this study.

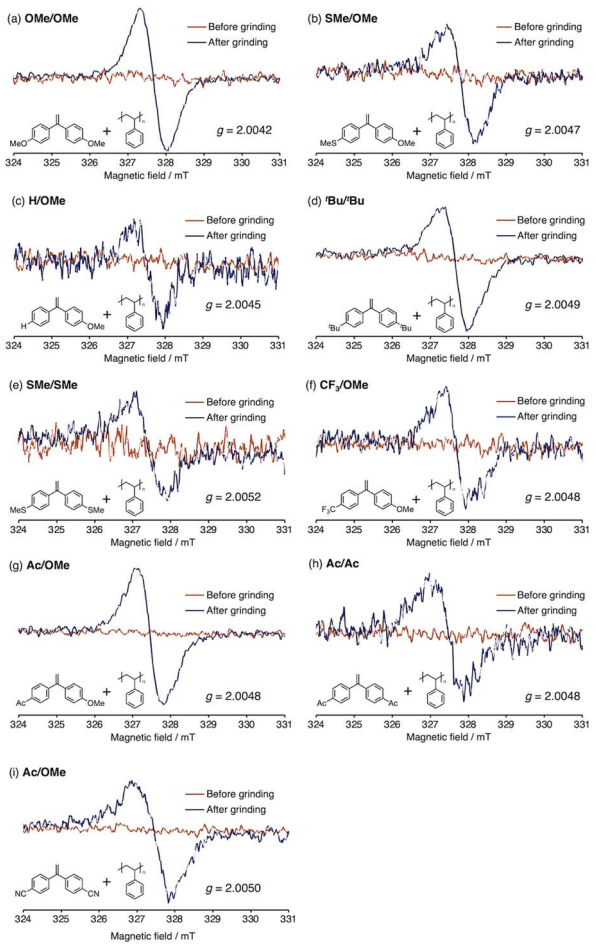

Fig. 8 EPR spectra of a mixture of PS and (a) **DAE-OMe/OMe**, (b) **DAE-SMe/OMe**, (c) **DAE-H/OMe**, (d) **DAE-^{t}Bu/^{t}Bu**, (e) **DAE-SMe/SMe**, (f) **DAE-CF$_3$/OMe**, (g) **DAE-Ac/OMe**, (h) **DAE-Ac/Ac** and (i) **DAE-Ac/OMe** before and after ball milling.

For all DAE derivatives, ball milling with PS resulted in the formation of the corresponding DAK derivatives. These results indicate that mechanoradical-mediated oxidative cleavage proceeds regardless of the electronic nature of the substituents (Fig. S37, S50–S57). The yields determined by ^{1}H NMR spectroscopy were below 35% for all substrates, and no systematic trend associated with substituent effects was observed (Fig. 7).

EPR measurements after ball milling revealed radical signals for all samples. All *g* values exceeded 2.004 and thus indicated that these species were oxygen-centred radicals (Fig. 8). The amount of generated radicals was comparable across most DAE derivatives, and no clear substituent effect was observed, consistent with the conversion data (Fig. 9).

Notably, the ^{1}H NMR spectra of the ground DAE derivatives bearing electron-withdrawing substituents showed a characteristic singlet at approximately 3.3 ppm, which could not be assigned to the corresponding DAK products. In contrast, this signal was absent for DAE derivatives without electron-withdrawing substituents. Similar trends have been reported previously for radical-mediated oxidation of aryl-substituted 1,1-disubstituted alkenes.[22] Because protons on oxirane rings are known to appear in this region, the newly observed signal was tentatively assigned to a 2,2-diaryloxirane (DAO) structure. To confirm this assignment, DAO derivatives were independently synthesized.

Guided by reported Corey–Chaykovsky-type epoxidation conditions,[50] the synthesis of three DAO derivatives bearing aromatic substituents with different electronic properties (**DAO-CN/CN**, **DAO-^{t}Bu/^{t}Bu**, and **DAO-OMe/OMe**) was examined to evaluate their relative stability. Initially, the synthesis of **DAO-CN/CN** bearing electron-withdrawing substituents on the aromatic rings was carried out, affording the desired product in 87% isolated yield. The ^{1}H NMR spectrum of the synthesized **DAO-CN/CN** was in excellent agreement with that of the newly observed unassigned signals in the spectrum obtained after grinding a mixture of **DAE-CN/CN** and PS. These results demonstrate that the mechanoradical-mediated oxidative cleavage of DAE derivatives bearing electron-withdrawing substituents affords the corresponding oxiranes in addition to ketones (Fig. 10).

Epoxidation of **DAE-^{t}Bu/^{t}Bu** bearing moderately electron-donating substituents gave peaks attributable to **DAO-^{t}Bu/^{t}Bu** in the ^{1}H NMR spectrum of the crude product. However, upon

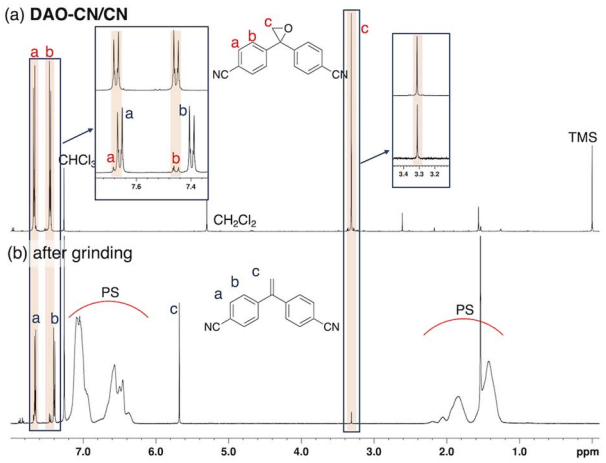

Fig. 10 ^{1}H NMR spectra of (a) **DAO-CN/CN** and (b) a mixture of PS and **DAE-CN/CN** after grinding ($CDCl_3$, 500 MHz).

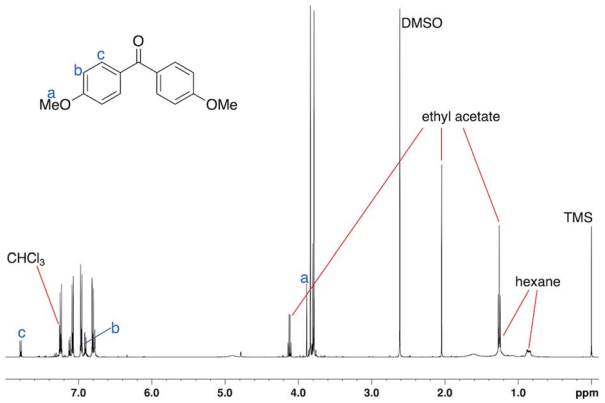

Fig. 12 ^{1}H NMR spectrum of the crude products of the Corey–Chaykovsky reaction of **DAE-OMe/OMe** ($CDCl_3$, 500 MHz).

standing as a solid powder under ambient conditions for 5 h, the signals of **DAO-^{t}Bu/^{t}Bu** disappeared, accompanied by an increase in spectral complexity in the aromatic region (Fig. 11). Similarly, for the ball-milled mixture of **DAE-^{t}Bu/^{t}Bu** and PS, a characteristic signal attributable to **DAO-^{t}Bu/^{t}Bu** was initially observed at 3.27 ppm immediately after milling, but it disappeared within several hours (Fig. S58).

Furthermore, the ^{1}H NMR spectrum of the crude product obtained from the Corey–Chaykovsky reaction of **DAE-OMe/OMe** showed no signals in the 3.0–3.5 ppm region characteristic of epoxy groups, indicating that **DAO-OMe/OMe** was not produced (Fig. 12). As observed for the crude product with ^{t}Bu groups, the aromatic region of the spectrum became more complex. These results suggest that DAO derivatives bearing electron-donating substituents are thermodynamically unstable and that the stability of DAO derivatives is strongly influenced by the electronic nature of the oxirane ring.

The relationship between the chemical shift of the β-carbon of DAE derivatives and the formation and persistence of DAO derivatives determined by ^{1}H NMR spectroscopy after ball milling is summarized in Table 2 (Fig. S58). DAE derivatives with an electron-rich β-carbon ($\delta \leq 112.58$ ppm) showed no detectable DAO-derived signals after ball milling with PS. DAE derivatives with a β-carbon of intermediate electron density ($\delta = 112.95$–113.49 ppm) exhibited transient DAO signals that disappeared within several hours. In contrast, for DAE derivatives with an electron-poor β-carbon ($\delta \geq 114.48$ ppm), DAO-derived signals remained detectable even several hours after milling. These results further support that DAO derivatives are increasingly stabilized as the electron density of the oxirane ring decreases.

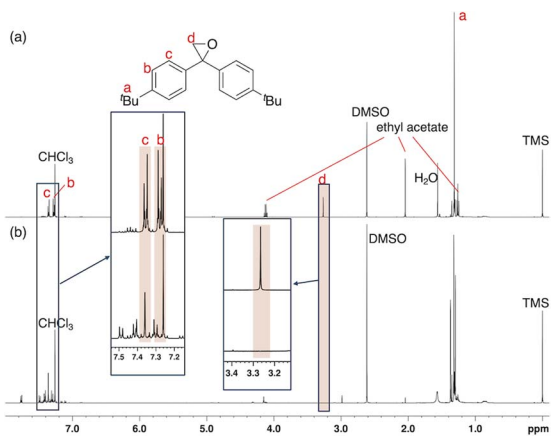

Fig. 11 ^{1}H NMR spectra of (a) the crude products of the Corey–Chaykovsky reaction with **DAO-^{t}Bu/^{t}Bu** and (b) the crude products left for 5 h ($CDCl_3$, 500 MHz).

Previous studies have proposed radical-mediated pathways in which DAO derivatives serve as intermediates en route to DAK formation during oxidative cleavage of DAE derivatives.[24] To examine whether such a pathway also operates under mechanochemical conditions, the reactivity of **DAO-CN/CN**, a thermodynamically stable DAO derivative, with mechanoradicals was investigated.

Ball milling of **DAO-CN/CN** alone resulted in no significant changes in the ^{1}H NMR spectrum (Fig. S62). Furthermore, ball milling of a mixture of **DAO-CN/CN** and PS also produced no appreciable changes in the spectrum (Fig. S60). These results indicate that, at least for DAO derivatives bearing electron-withdrawing substituents, conversion from DAO to DAK *via* mechanoradical-mediated pathways does not occur.

On the basis of all the findings obtained, a plausible pathway for DAO formation during the mechanoradical-mediated oxidation of DAE derivatives is proposed as shown in Scheme 3. In analogy with literature precedents for peroxyl-radical-mediated alkene oxidation, oxygenated radical intermediates generated under the aerobic mechanochemical conditions may react with DAE derivatives to form peroxide-type intermediates, from which DAO derivatives may be produced. Earlier gas-phase studies proposed epoxide formation as a major outcome of peroxyl-radical addition to alkenes, whereas a more recent study under atmospheric conditions suggests that non-epoxide pathways can also operate, depending on the reaction conditions.[51–53]

Table 2 Oxirane generation immediately after grinding and approximately 3 hours later[a]

R^1	OMe	SMe	H	^{t}Bu	SMe	CF_3	Ac	Ac	CN
R^2	OMe	OMe	OMe	^{t}Bu	SMe	OMe	OMe	Ac	CN
δ/ppm	111.67	112.58	112.95	113.16	113.49	114.48	114.62	117.61	118.54
Right after grinding	−	−	+	+	+	+	+	+	+
3 hours later	−	−	−	−	−	+	+	+	+

[a] + indicates detected; − indicates not detected.

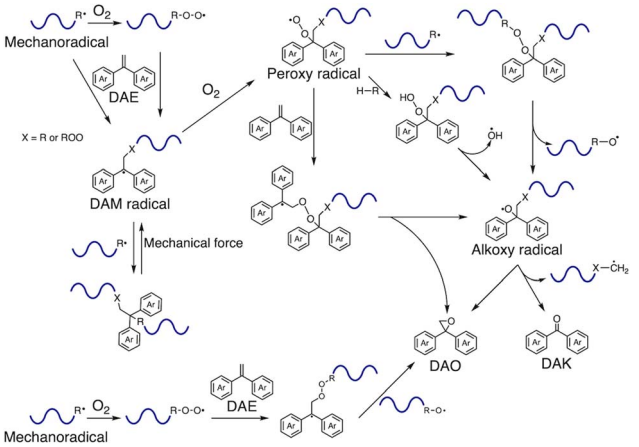

Scheme 3 Plausible mechanism for the mechanoradical-mediated formation of DAO derivatives.

Accordingly, DAO formation in the present system may proceed through peroxide- and/or alkoxy-radical pathways under mechanochemical conditions. Importantly, our control experiments indicate that stable DAO derivatives are unlikely to act as obligatory intermediates in the formation of DAK under the present conditions. Instead, DAO and DAK are more plausibly formed through divergent pathways from common oxygenated radical intermediates.

Conclusions

In summary, we have demonstrated that polymer-derived mechanoradicals generated by chain scission can serve as effective initiators for the oxidative cleavage of 1,1-disubstituted alkenes using molecular oxygen as the oxidant. Ball milling of PS in the presence of DAE derivatives led to polymer chain cleavage accompanied by the formation of DAK derivatives, the oxidative cleavage products of DAE. EPR spectroscopy revealed the formation of oxygen-centered radicals, suggesting a reaction pathway in which polymer-derived mechanoradicals initially add to DAE derivatives, followed by reaction with atmospheric oxygen during the oxidative cleavage.

Investigation using PMMA further demonstrated that mechanoradical-mediated oxidative cleavage proceeds regardless of the polymer identity, while indicating that the amount of generated mechanoradicals influences the overall reaction efficiency. Moreover, GPC analysis using UV detection revealed that mechanoradicals can be partially incorporated into polymer chains *via* addition of the mechanoradical to DAE derivatives.

Collectively, these results demonstrate that polymer-derived mechanoradicals can trigger oxidative transformations of DAE derivatives through radical addition processes and serve as an effective tool for probing radical oxidation mechanisms in the solid state. This work establishes a versatile platform for elucidating elementary steps of radical reactions using solid-state mechanochemistry and is expected to contribute to the future development of mechanochemical reaction control and mechanistic analysis.

Author contributions

A. K.: writing – original draft, methodology, investigation, formal analysis, data curation. T. Y.: methodology, formal analysis. H. S.: methodology, formal analysis. A. T.: writing – review & editing, supervision, methodology, formal analysis, conceptualization. H. O.: writing – review & editing, supervision, project administration, resources, funding acquisition, formal analysis.

Conflicts of interest

There are no conflicts to declare.

Data availability

Data supporting this article have been included in the supplementary information (SI). Supplementary information: synthetic procedures of compounds and their NMR and IR data, GPC profiles before and after grinding, and details of the experiments. See DOI: https://doi.org/10.1039/d6mr00040a.

Acknowledgements

This work was supported by KAKENHI grant 21H04689 (to H. O.) from the Japan Society for the Promotion of Science (JSPS). This work was supported by JST SPRING, Japan Grant Number JPMJSP2180 (to A. K.).

Notes and references

1 A. Rajagopalan, M. Lara and W. Kroutil, *Adv. Synth. Catal.*, 2013, **355**, 3321–3335.

2 C. Tang, X. Qiu, Z. Cheng and N. Jiao, *Chem. Soc. Rev.*, 2021, **50**, 8067–8101.
3 P. Spannring, P. C. A. Bruijnincx, B. M. Weckhuysen and R. J. M. Klein Gebbink, *Catal. Sci. Technol.*, 2014, **4**, 2182.
4 W. A. Hussain and M. Parasram, *Synthesis*, 2024, **56**, 1775–1786.
5 G. Urgoitia, R. SanMartin, M. T. Herrero and E. Domínguez, *ACS Catal.*, 2017, **7**, 3050–3060.
6 R. Criegee, *Angew. Chem., Int. Ed. Engl.*, 1975, **14**, 745–752.
7 S. Lai and D. G. Lee, *Synthesis*, 2001, **11**, 1645–1648.
8 B. Alcaide, P. Almendros and J. M. Alonso, *Tetrahedron Lett.*, 2003, **44**, 8693–8695.
9 L. G. Arini, P. Szeto, D. L. Hughes and R. A. Stockman, *Tetrahedron Lett.*, 2004, **45**, 8371–8374.
10 T. J. Fisher and P. H. Dussault, *Tetrahedron*, 2017, **73**, 4233–4258.
11 V. Piccialli, *Molecules*, 2014, **19**, 6534–6582.
12 T. Patra and T. Wirth, *Angew. Chem., Int. Ed.*, 2022, **61**, e202213772.
13 Z. Huang, R. Guan, M. Shanmugam, E. L. Bennett, C. M. Robertson, A. Brookfield, E. J. L. McInnes and J. Xiao, *J. Am. Chem. Soc.*, 2021, **143**, 10005–10013.
14 R. Lin, F. Chen and N. Jiao, *Org. Lett.*, 2012, **14**, 4158–4161.
15 Z. Zhang, W. Chen and J. Luo, *Tetrahedron Lett.*, 2020, **61**, 152527.
16 S. Eşsiz and U. Bozkaya, *J. Org. Chem.*, 2020, **85**, 10136–10142.
17 T. Wang and N. Jiao, *J. Am. Chem. Soc.*, 2013, **135**, 11692–11695.
18 Y. Deng, X.-J. Wei, H. Wang, Y. Sun, T. Noël and X. Wang, *Angew. Chem., Int. Ed.*, 2017, **56**, 832–836.
19 B. Xiong, X. Zeng, S. Geng, S. Chen, Y. He and Z. Feng, *Green Chem.*, 2018, **20**, 4521–4527.
20 X. Wang, Y. Li and Z. Li, *Catal. Sci. Technol.*, 2021, **11**, 1000–1006.
21 G.-Z. Wang, X.-L. Li, J.-J. Dai and H.-J. Xu, *J. Org. Chem.*, 2014, **79**, 7220–7225.
22 H. Aman, W.-H. Chiu, P.-H. Liu and G. J. Chuang, *New J. Chem.*, 2021, **45**, 20103–20106.
23 S. Eşsiz and U. Bozkaya, *Org. Biomol. Chem.*, 2021, **19**, 9483–9490.
24 Z. Cheng, W. Jin and C. Liu, *Org. Chem. Front.*, 2019, **6**, 841–845.
25 K.-J. Liu, J.-H. Deng, T.-Y. Zeng, X.-J. Chen, Y. Huang, Z. Cao, Y.-W. Lin and W.-M. He, *Chin. Chem. Lett.*, 2020, **31**, 1868–1872.
26 T. Yu, M. Guo, S. Wen, R. Zhao, J. Wang, Y. Sun, Q. Liu and H. Zhou, *RSC Adv.*, 2021, **11**, 13848–13852.
27 Y.-X. Chen, J.-T. He, M.-C. Wu, Z.-L. Liu, K. Tang, P.-J. Xia, K. Chen, H.-Y. Xiang, X.-Q. Chen and H. Yang, *Org. Lett.*, 2022, **24**, 3920–3925.
28 C. Wang, C.-L. Sun and R. Boulatov, *Chem. Commun.*, 2024, **60**, 10629–10641.
29 A. Rizzo and G. I. Peterson, *Prog. Polym. Sci.*, 2024, **159**, 101900.
30 T. Matsuda, R. Kawakami, R. Namba, T. Nakajima and J. P. Gong, *Science*, 2019, **363**, 504–508.
31 K. Seshimo, H. Sakai, T. Watabe, D. Aoki, H. Sugita, K. Mikami, Y. Mao, A. Ishigami, S. Nishitsuji, T. Kurose, H. Ito and H. Otsuka, *Angew. Chem., Int. Ed.*, 2021, **60**, 8406–8409.
32 Z. J. Wang, W. Li, X. Li, T. Nakajima, M. Rubinstein and J. P. Gong, *Nat. Mater.*, 2025, **24**, 607–614.
33 K. Kubota, N. Toyoshima, D. Miura, J. Jiang, S. Maeda, M. Jin and H. Ito, *Angew. Chem., Int. Ed.*, 2021, **60**, 16003–16008.
34 R. Schwarz and C. E. Diesendruck, *Adv. Sci.*, 2023, **10**, 2304571.
35 H. Xie, J. Wang, Z. Lou, L. Hu, S. Segawa, X. Kang, W. Wu, Z. Luo, R. T. K. Kwok, J. W. Y. Lam, J. Zhang and B. Z. Tang, *J. Am. Chem. Soc.*, 2024, **146**, 18350–18359.
36 T. Yamamoto, S. Kato, D. Aoki and H. Otsuka, *Angew. Chem., Int. Ed.*, 2021, **60**, 2680–2683.
37 Q. Huang, O. Hassager and J. Madsen, *Macromolecules*, 2022, **55**, 9431–9441.
38 T. Yamamoto, A. Takahashi and H. Otsuka, *RSC Mechanochem.*, 2024, **1**, 63–68.
39 T. Yamamoto, D. Aoki, K. Mikami and H. Otsuka, *RSC Mechanochem.*, 2024, **1**, 181–188.
40 K. Kubota, J. Jiang, Y. Kamakura, R. Hisazumi, T. Endo, D. Miura, S. Kubo, S. Maeda and H. Ito, *J. Am. Chem. Soc.*, 2024, **146**, 1062–1070.
41 S. L. James, C. J. Adams, C. Bolm, D. Braga, P. Collier, T. Friščić, F. Grepioni, K. D. M. Harris, G. Hyett, W. Jones, A. Krebs, J. Mack, L. Maini, A. G. Orpen, I. P. Parkin, W. C. Shearouse, J. W. Steed and D. C. Waddell, *Chem. Soc. Rev.*, 2011, **41**, 413–447.
42 Y. Chen, G. Mellot, D. van Luijk, C. Creton and R. P. Sijbesma, *Chem. Soc. Rev.*, 2021, **50**, 4100–4140.
43 J. F. Reynes, F. Leon and F. García, *ACS Org. Inorg. Au*, 2024, **4**, 432–470.
44 S. Arfelis, A. I. Martín-Perales, R. Nguyen, A. Pérez, I. Cherubin, C. Len, I. Malpartida, A. Bala and P. Fullana-i-Palmer, *Heliyon*, 2024, **10**, e34655.
45 A. B. Chetry, *J. Chem. Res.*, 2025, **49**, 16.
46 E. Jung, M. Cho, G. I. Peterson and T.-L. Choi, *Macromolecules*, 2024, **57**, 3131–3137.
47 J. Mack and M. Shumba, *Green Chem.*, 2007, **9**, 328–330.
48 V. Štrukil, D. Margetić, M. D. Igrc, M. Eckert-Maksić and T. Friščić, *Chem. Commun.*, 2012, **48**, 9705–9707.
49 Z. Zhang, H.-H. Wu and Y.-J. Tan, *RSC Adv.*, 2013, **3**, 16940–16944.
50 A. K. Pandey and P. Banerjee, *Asian J. Org. Chem.*, 2016, **5**, 360–366.
51 M. S. Stark, *J. Phys. Chem. A*, 1997, **101**, 8296–8301.
52 M. S. Stark, *J. Am. Chem. Soc.*, 2000, **122**, 4162–4170.
53 B. Nozière, O. Durif, E. Dubus, S. Kylington, Å. Emmer, F. Fache, F. Piel and A. Wisthaler, *Phys. Chem. Chem. Phys.*, 2023, **25**, 7772–7782.